LPT-Orsay-15-80

Nonthermal dark matter models and signals

Hiroshi Okada,[1,2,*] Yuta Orikasa,[1,3,†] and Takashi Toma[4,‡]

[1] *School of Physics, KIAS, Seoul 130-722, Korea*

[2] *Physics Division, National Center for Theoretical Sciences, Hsinchu, Taiwan 300*

[3] *Department of Physics and Astronomy, Seoul National University, Seoul 151-742, Korea*

[4] *Laboratoire de Physique Théorique, CNRS, Univ. Paris-Sud, Université Paris-Saclay, 91405 Orsay, France*

(Dated: March 7, 2016)

arXiv:1511.01018v3 [hep-ph] 4 Mar 2016

Abstract

Many experiments exploring weakly interacting massive particles (WIMPs) such as direct, indirect and collider searches have been carried out until now. However, a clear signal of a WIMP has not been found yet and it makes us to suspect that WIMPs are questionable as a dark matter candidate. Taking into account this situation, we propose two models in which dark matter relic density is produced by decay of a metastable particle. In the first model, the metastable particle is a feebly interacting massive particle, which is the so-called FIMP produced by freeze-in mechanism in the early universe. In the second model, the decaying particle is thermally produced the same as the usual WIMP. However decay of the particle into dark matter is led by a higher dimensional operator. As a phenomenologically interesting feature of nonthermal dark matter discussed in this paper, a strong sharp gamma-ray emission as an indirect detection signal occurs due to internal bremsstrahlung, although some parameter space has already been ruled out by this process. Moreover combining other experimental and theoretical constraints such as dark matter relic density, big bang nucleosynthesis, collider, gamma-rays and perturbativity of couplings, we discuss the two nonthermal DM models.

Keywords: Non-thermal dark matter, Gamma-rays, Internal bremsstrahlung, Freeze-in mechanism

*Electronic address: macokada3hiroshi@gmail.com

†Electronic address: orikasa@kias.re.kr

‡Electronic address: takashi.toma@th.u-psud.fr

I. INTRODUCTION

Exploring the nature of dark matter (DM) is one of the most important issues to provide an appropriate prescription to improve the standard model (SM). The most promising DM candidate is weakly interacting massive particles (WIMPs) whose mass is predicted to be the order of 10 GeV to 10 TeV, and many experiments are focusing on WIMP searches. However in spite of great effort of experiments for WIMP search such as direct, indirect and collider searches, no positive evidence for WIMPs is found up to the present. Although the gamma-ray excess from the galactic center has been claimed and could be explained by WIMP with its typical annihilation cross section $\sigma v_{\rm rel} \sim 10^{-26}$ cm^3/s [1–5], it is strongly constrained by nondetection of such a gamma-ray excess from the other galaxies. In particular, the constraint on the WIMP annihilation cross section from dwarf spheroidal galaxies is the strongest for specific channels [6]. For direct detection experiments, the elastic cross section with a nucleon is strongly constrained, and more and more parameter space of the WIMP is excluded [7, 8], while this strong bound may be evaded by considering the WIMP interacting with quarks via a pseudoscalar, leptophilic DM and resonance region in Higgs portal models. Even for collider searches, any collider signal for the WIMP has not been found yet at the LHC [9, 10]. This may imply that DM in the universe is not composed of the traditional WIMP candidate, and motivate us to consider non-WIMP DM scenarios. There are a lot of DM candidates other than the WIMP, for example axion [11–13], asymmetric DM [14–16], sterile neutrino [17, 18], strongly interacting massive particle [19–22].

In this paper, we construct two kinds of nonthermal DM models.[1] In both models, the DM particle is produced by decay of a metastable particle after freeze-out of DM, but the production of the decaying particle is different. Such nonthermally produced DM particles have a phenomenologically interesting feature, which is a strong signal for indirect detection. For traditional thermally produced DM, the interaction strength of WIMPs is fixed by the annihilation cross section in order to accommodate the correct relic density observed by PLANCK [34]. Thus in this case, the signal strength for indirect DM detection is also determined. On the other hand, for nonthermally produced DM like our case, the strength of the interactions is not fixed and can be larger than the interaction of WIMPs since the

[1] Some related nonthermal DM production mechanisms have been discussed in Refs. [13, 23–33].

DM relic density is mainly generated by the metastable particle decay.

In the first model, a new decaying particle has only dimension 5 operators and the interactions are highly suppressed. Namely this particle can be a feebly interacting massive particle (FIMP) [35],[2] and is produced in the early universe by so-called freeze-in scenario. The DM particle is nonthermally produced by the decay of FIMP. In the second model, both the DM particle and the decaying particle can be thermally produced at the beginning. Then the decaying particle can be metastable since the interactions of the particle are highly suppressed by dimension 5 operators. The heavier particle decays into the DM particle through the dimension 5 operators after DM freeze-out. In this way, the DM relic density can be reproduced non-thermally. In addition, neutrino masses are generated at one-loop level in the second model. We discuss which parameter space in the two models is allowed by some experimental and theoretical constraints and is favored to see the nonthermal DM signal.

This paper is organized as follows. In Sec. II and Sec. III, we discuss the first model (Model I) and the second model (Model II) respectively, in which we formulate the relevant Lagrangian, the coupled Boltzmann equation for the DM relic density, neutrino masses, and analyze the DM signature. Summary and conclusion are given in Sec. IV.

II. THE MODEL I

A. Model setup

We consider a model with a discrete symmetry $\mathbb{Z}_4 \times \mathbb{Z}_2$. The new particle contents and their charge assignments are shown in Table I where all the SM particles are neutral under the $\mathbb{Z}_4 \times \mathbb{Z}_2$ symmetry. These discrete $\mathbb{Z}_N$ symmetries could be understood as a remnant symmetry of a $U(1)$ gauge symmetry which comes from string theory [38]. As in Table I, we add two gauge singlet right-handed fermions X and N, a charged singlet scalar S^+ and a neutral singlet scalar S^0 to the SM. The kinetic terms of the new particles and the Majorana mass terms of the new fermions are given by

$$\mathcal{L}_K = \frac{1}{2}\overline{X^c}\left(i\partial\!\!\!/ - m_X\right)X + \frac{1}{2}\overline{N^c}\left(i\partial\!\!\!/ - m_N\right)N + \left|\partial_\mu S^0\right|^2 + \left|D_\mu S^+\right|^2, \tag{II.1}$$

[2] The same mechanism has been discussed in a concrete model previously [36, 37].

	X	N	S^0	S^+
$(SU(2)_L, U(1)_Y)$	$(\mathbf{1}, 0)$	$(\mathbf{1}, 0)$	$(\mathbf{1}, 0)$	$(\mathbf{1}, 1)$
$(\mathbb{Z}_4, \mathbb{Z}_2)$	$(-1, -)$	$(+1, -)$	$(\pm i, +)$	$(+1, -)$
Spin	1/2	1/2	0	0

TABLE I: New particle contents of Model I and their charge assignments under $SU(2)_L \times U(1)_Y \times \mathbb{Z}_4 \times \mathbb{Z}_2$, where all the SM particles are neutral under $\mathbb{Z}_4 \times \mathbb{Z}_2$.

where the covariant derivative for S^+ is defined by $D_\mu \equiv \partial_\mu + i g_Y B_\mu$ with the $U(1)_Y$ gauge coupling g_Y and the $U(1)_Y$ field B_μ. Under the charge assignment, the relevant Lagrangian for Yukawa sector up to dimension 5 operators is given by

$$\begin{aligned}
\mathcal{L}_Y \;=\; & -y_N S^+ \overline{N^c} e_R - y_\ell H \overline{L_L} e_R - \frac{\lambda_\nu}{4\Lambda}(H H \overline{L_L^c} L_L) \\
& - \frac{\lambda_1}{2\Lambda}(\overline{X^c} X)|H|^2 - \frac{\lambda_2}{2\Lambda}(\overline{N^c} N)|H|^2 - \frac{\lambda_3}{2\Lambda}(\overline{X^c} N)(S^{0\dagger})^2 - \frac{\lambda_4}{2\Lambda}(\overline{X^c} X)|S^0|^2 \\
& - \frac{\lambda_5}{2\Lambda}(\overline{X^c} X)|S^+|^2 - \frac{\lambda_6}{2\Lambda}(\overline{N^c} N)|S^0|^2 - \frac{\lambda_7}{2\Lambda}(\overline{N^c} N)|S^+|^2 + \text{H.c.},
\end{aligned} \tag{II.2}$$

where Λ is a cutoff scale of the model, H is the Higgs doublet, L_L and e_R are the $SU(2)_L$ doublet and singlet SM lepton fields.[3] In general, the Yukawa coupling y_N is possible for all the leptons, however we consider the dominant coupling with electron for simplicity. The charged lepton masses can be induced by the term $y_\ell \overline{L_L} H e_R$ as same as the SM, and the neutrino masses can be generated by the Weinberg operator with the λ_ν coupling in Eq. (II.2) [39]. From the Weinberg operator, the cutoff scale Λ is estimated as $\Lambda \sim 10^{14} \lambda_\nu$ GeV where the neutrino mass scale is assumed to be $m_\nu \sim 0.1$ eV.

Only the SM Higgs field denoted as H and the new singlet scalar S^0 should have vacuum expectation values (VEVs), which are symbolized by $\langle H \rangle = v/\sqrt{2} \approx 174$ GeV and $\langle S^0 \rangle = v'/\sqrt{2}$ respectively. The $\mathbb{Z}_4$ symmetry is spontaneously broken by the VEV of S^0, whereas the $\mathbb{Z}_2$ symmetry remains even after the electroweak symmetry breaking. Hence the $\mathbb{Z}_2$ symmetry assures the stability of DM, and we can identify the Majorana fermion X or N as a DM candidate since they are neutral and have the $\mathbb{Z}_2$ odd charge. The Majorana fermions X and N mix with each other due to the VEV of S^0 via the coupling λ_3, and the mixing

[3] Notice here that there exists a dimension 5 operator $\overline{X} \sigma^{\mu\nu} X F_{\mu\nu}$ if the fermion X is a Dirac field.

mass is given by $m_{XN} = \lambda_3 v'^2/(2\Lambda)$. However since the mixing occurs with the dimension 5 operator and the cutoff scale Λ is expected to be very large in order to obtain the appropriate neutrino mass scale with $\mathcal{O}(1)$ dimensionless couplings λ_ν, we can naturally expect that the mixing component is very small compared to the diagonal elements and one can regard that the Majorana fermions X and N are almost mass eigenstates themselves. The SM Higgs boson H^0 and S^0 mix after the electroweak symmetry breaking and the mixing angle is constrained by experiments [40]. However this is not relevant to our work.

B. Dark matter

1. *Freeze-in scenario*

In this model, one of the Majorana fermions X and N can be a DM candidate depending on the mass hierarchy. Since all the interactions of the fermion X are suppressed by the cutoff scale Λ as one can see from Eq. (II.2), the fermion X may not be suitable as a standard thermally produced DM candidate. However, because of the highly suppressed interactions, the fermion X may never reach to thermal equilibrium with the SM particles. In this case, the production of the fermion X occurs by so-called freeze-in mechanism [33, 35]. Although the nonthermally produced X itself can be a DM candidate, it would be difficult to search such a DM candidate since X has only extremely suppressed interactions. The most phenomenologically interesting possibility would be a scenario that the Majorana fermion N is the DM candidate which is reproduced by the decay of the fermion X after the DM freeze-out. Because of the nonthermal production mechanism of DM N, one can expect a larger indirect detection signal of DM since the interactions of nonthermally produced DM can generally be larger than traditional thermally produced DM. Thus we will discuss this scenario below.

The following coupled Boltzmann equation for N and X should be solved in order to compute the DM relic density

$$\begin{aligned}\frac{dY_X}{dx} &= \frac{1}{sxH}\left(\frac{g_X m_X^2 m_N \Gamma_X}{2\pi^2 x}\right) K_1\left(\frac{m_X}{m_N}x\right) - \frac{\Gamma_X Y_X}{xH},\\ \frac{dY_N}{dx} &= -\frac{s\langle\sigma_{\rm eff} v_{\rm rel}\rangle}{xH}\left(Y_N^2 - Y_N^{\rm eq2}\right) + \frac{\Gamma_X Y_X}{xH},\end{aligned} \tag{II.3}$$

where $g_X = 2$ is the degree of freedom of the Majorana fermion X, $x = m_N/T$ is a di-

mensionless parameter with the temperature of the universe, Y_N and Y_X are defined by $Y_N \equiv n_N/s$ and $Y_X \equiv n_X/s$ with the number densities n_N, n_X and the entropy density s, $Y_N^{\rm eq}$ represents the number density of N in thermal equilibrium, H is the Hubble parameter, and K_1 is the modified Bessel function of the second kind with the order 1. The first term including the modified Bessel function in Eq. (II.3) implies the X production due to the inverse decay process $NS^0 \to X$ via the dimension 5 operator with λ_3 where $m_X > m_N + m_{S^0}$ is assumed. One may think that the scattering processes induced by the other dimension 5 operators in Eq. (II.2) should also be taken into account and be added to the coupled Boltzmann equation. In fact if the reheating temperature of the universe is high enough compared to the following criterion Eq. (II.4), the time evolution of the number density of X is dominantly determined by the scattering processes. While if the reheating temperature is not so high, the time evolution is almost determined by the inverse decay process we included. Thus the assumption that the inverse decay process is dominant for freeze-in mechanism gives a constraint on reheating temperature. The constraint on the reheating temperature is roughly estimated as [35]

$$T_R \lesssim \frac{3\pi^2 v'^2}{m_X}. \tag{II.4}$$

For example, when $m_X = 10$ TeV, $v' = 3$ TeV, the upper bound of the reheating temperature is derived as $T_R \lesssim 27$ TeV. More general analysis for treatment of nonrenormalizable operators has been discussed in Ref. [41].

The fermion X can decay as $X \to NS^0$ via the coupling λ_3, and the decay width Γ_X is computed as

$$\Gamma_X = \frac{\lambda_3^2 m_X}{16\pi}\left(\frac{v'}{\Lambda}\right)^2 \sqrt{1-\left(\frac{m_N}{m_X}+\frac{m_{S^0}}{m_X}\right)^2}\sqrt{1-\left(\frac{m_N}{m_X}-\frac{m_{S^0}}{m_X}\right)^2}\left[\left(1-\frac{m_N}{m_X}\right)^2 - \frac{m_{S^0}^2}{m_X^2}\right]. \tag{II.5}$$

Thus one can obtain the rough estimation for $m_X \gg m_N, m_{S^0}$ as

$$\Gamma_X \sim 2\times 10^{-20}\left(\frac{\lambda_3}{1}\right)^2\left(\frac{m_X}{10\ \text{TeV}}\right)\left(\frac{v'}{1\ \text{TeV}}\right)^2\left(\frac{10^{14}\ \text{GeV}}{\Lambda}\right)^2\ \text{GeV}. \tag{II.6}$$

The DM annihilation cross section $\sigma_{NN} v_{\rm rel}$ can be expanded by the DM relative velocity $v_{\rm rel}$ as usual way. In this model, the DM annihilation channel is only $NN \to e_R\overline{e_R}$ via the Yukawa coupling y_N, and the concrete expression of the expansion is given by

$$\sigma_{NN} v_{\rm rel} = \frac{y_N^4}{48\pi m_N^2}\frac{1+\mu_N^2}{(1+\mu_N)^4} v_{\rm rel}^2, \tag{II.7}$$

with $\mu_N = m_{S^+}^2/m_N^2$. The first term of the expansion which corresponds to s-wave does not exist because of chiral suppression. The thermally averaged cross section $\langle\sigma_{NN}v_{\rm rel}\rangle$ is given by replacing $v_{\rm rel}^2 \to 6/x$ in Eq. (II.7). In addition to the DM annihilation, the coannihilation processes with $S^\pm$ should be taken into account since we will consider the degenerate mass $m_N \approx m_{S^+}$ in order to obtain an interesting DM signal in indirect detection. The coannihilation cross sections and self-annihilation cross sections of $S^\pm$ for each channel are computed as

$$\sigma v_{\rm rel}(S^+S^- \to \gamma\gamma) = \frac{e^4}{8\pi m_N^2}\left(1-\frac{7}{12}v_{\rm rel}^2\right), \tag{II.8}$$

$$\sigma v_{\rm rel}(S^+S^- \to \gamma Z) = \frac{e^4\tan^2\theta_W}{4\pi m_N^2}\left(1-\frac{7}{12}v_{\rm rel}^2\right), \tag{II.9}$$

$$\sigma v_{\rm rel}(S^+S^- \to ZZ) = \frac{e^4\tan^4\theta_W}{8\pi m_N^2}\left(1-\frac{7}{12}v_{\rm rel}^2\right), \tag{II.10}$$

$$\sigma v_{\rm rel}(S^+S^- \to W^+W^-) = \frac{e^4}{1536\pi m_N^2}\frac{m_Z^4}{m_W^4}v_{\rm rel}^2, \tag{II.11}$$

$$\sum_f \sigma v(S^+S^- \to f\bar{f}) = \left(\frac{1}{768}\frac{5e^4}{\cos^4\theta_W} - \frac{1}{96}\frac{y_N^2e^2}{\cos^2\theta_W} + \frac{y_N^4}{192}\right)\frac{v_{\rm rel}^2}{\pi m_N^2}, \tag{II.12}$$

$$\sigma v_{\rm rel}(S^\pm S^\pm \to e^\pm e^\pm) = \frac{y_N^4}{16\pi m_N^2}\left(1-\frac{v_{\rm rel}^2}{3}\right), \tag{II.13}$$

$$\sigma v_{\rm rel}(S^\pm N \to e^\pm\gamma) = \frac{y_N^2e^2}{64\pi m_N^2}\left(1-\frac{v_{\rm rel}^2}{4}\right), \tag{II.14}$$

$$\sigma v_{\rm rel}(S^\pm N \to e^\pm Z) = \frac{y_N^2e^2\tan^2\theta_W}{64\pi m_N^2}\left(1-\frac{v_{\rm rel}^2}{4}\right), \tag{II.15}$$

where f in Eq. (II.12) represents the SM fermions, the SM Yukawa couplings and the $|S^+|^2|H|^2$ coupling are neglected for simplicity, and the mass relations $m_W, m_Z \ll m_N$ and $\mu_N = 1$ are assumed. The co-annihilation cross section for the process $S^\pm N \to \nu W^\pm$ is proportional to m_e^2/m_W^2. In addition, the cross section for $S^\pm N \to he^\pm$ is written by the electron Yukawa coupling where h is the SM-like Higgs boson with $m_h = 125$ GeV. Thus these contributions are negligible. We have computed the above analytical formulas with FEYNCALC [42], and have numerically checked with CALCHEP [43, 44]. The general formula of the effective cross section including coannihilation processes is given by [45]

$$\sigma_{\rm eff}v_{\rm rel} = \sum_{i,j}\frac{g_ig_j}{g_{\rm eff}^2}\sigma_{ij}v_{\rm rel}\,(1+\Delta_i)^{3/2}\,(1+\Delta_j)^{3/2}\,e^{-x(\Delta_i+\Delta_j)}, \tag{II.16}$$

where i,j imply the DM particle (N) and the degenerate particles with DM ($S^\pm$), $\Delta_i \equiv (m_i - m_N)/m_N$, g_i is the degree of freedom of the particle i and the effective degree of

freedom $g_{\rm eff}$ is given by

$$g_{\rm eff} = \sum_i g_i \left(1+\Delta_i\right)^{3/2} e^{-x\Delta_i}. \tag{II.17}$$

In our case with $\mu_N = 1$, the effective cross section including all the above processes is simply given by

$$\sigma_{\rm eff} v_{\rm rel} = \frac{\sigma_{NN} v_{\rm rel}}{4} + \frac{\sigma_{S^\pm S^\mp} v_{\rm rel}}{8} + \frac{\sigma_{S^\pm S^\pm} v_{\rm rel}}{8} + \frac{\sigma_{N S^\pm} v_{\rm rel}}{2}, \tag{II.18}$$

where $\sigma_{S^\pm S^\mp} v_{\rm rel}$ is defined by the sum of Eq. (II.8), (II.9), (II.10), (II.11) and (II.12), $\sigma_{S^\pm S^\pm} v_{\rm rel}$ is the contribution of $S^\pm S^\pm \to e^\pm e^\pm$ given by Eq. (II.13), and $\sigma_{N S^\pm} v_{\rm rel}$ is given by the sum of Eq. (II.14) and (II.15). The thermally averaged effective cross section $\langle \sigma_{\rm eff} v_{\rm rel} \rangle$ is needed to solve the Boltzmann equation Eq. (II.3).

2. *Numerical result*

The coupled Boltzmann equation in Eq. (II.3) combined with the X decay width Eq (II.5) and the DM cross section Eq. (II.18), is numerically solved. Figure 1 shows the numerical results for $\mu_N = 1$ in Γ_X-y_N plane where the decaying Majorana fermion mass m_X is fixed to $m_X = 1$ TeV in the left panel and 10 TeV in the right panel. Each red, green and blue colored line satisfies the observed relic density $\Omega h^2 \approx 0.12$ for the fixed DM mass $m_N = 200, 300, 500$ GeV in the left panel and $m_N = 500, 1000, 3000$ GeV in the right panel respectively.

The black colored region represents $m_N > m_X$, thus the decay of X does not occur. The green colored upper region is excluded by the conservative perturbativity of the Yukawa coupling $y_N \geq \sqrt{4\pi}$. If the lifetime of X is as long as $\tau_X \sim 0.1$ s corresponding to $\Gamma_X \sim 10^{-23}$ GeV, the X decay may affect to the successful big bang nucleosynthesis (BBN) [46, 47]. Therefore the conservative limit for the lifetime $\tau_X \lesssim 0.1$ s is imposed in our analysis, and the left orange region of Fig. 1 shown with BBN limit is excluded by this constraint.

The light-red and violet colored regions in the center of each figure are excluded by the gamma-ray and LEP experiment respectively [48, 49]. For the LEP bound, we take a conservative lower bound for the charged scalar $m_{S^+} \geq 100$ GeV which corresponds to $m_N \geq 100$ GeV since the mass ratio is fixed to be $\mu_N = 1$. For the gamma-ray constraint, we take into account internal bremsstrahlung of Majorana DM $NN \to e\bar{e}\gamma$ [50–57].[4] Indeed

[4] Internal bremsstrahlung has also been discussed for scalar DM coupling with a vectorlike fermion [58–61].

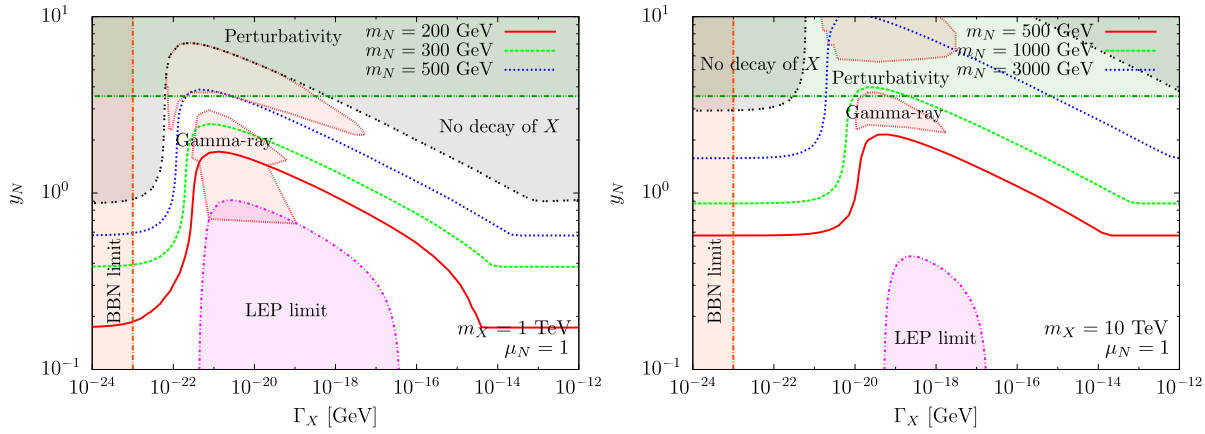

FIG. 1: Allowed parameter space in Γ_X-y_N plane where the mass ratio is fixed as $\mu_N = 1$ and the mass of the Majorana fermion X is taken to be $m_X = 1$ TeV in the left panel and to be $m_X = 10$ TeV in the right panel. The red, green, and blue colored lines imply the contours satisfying the observed relic density $\Omega h^2 \approx 0.12$ for fixed DM masses. The white region is allowed by all the current experimental and theoretical bounds.

in our case, this process is promising channel for indirect detection of DM, since the DM self-annihilation channel is chirally suppressed with $v_{\rm rel} \sim 10^{-3}$ as in Eq. (II.7). For the case of thermal DM, this cross section is fixed to obtain the observed DM thermal relic density, and cannot be so large. However in our nonthermal DM model, it can be large enough to be detectable in the near future since we can take a larger Yukawa coupling y_N being consistent with the observed DM relic density. The gamma-ray spectrum coming from internal bremsstrahlung $NN \to e\bar{e}\gamma$ especially becomes very sharp when the mass ratio μ_N is close to 1 and may give a strong constraint on our model. That is why the mass ratio μ_N is fixed to be $\mu_N = 1$ in our analysis in order to obtain a sharp gamma-ray spectrum of internal bremsstrahlung. The total cross section for the process is given by

$$\sigma_{e\bar{e}\gamma} v_{\rm rel} = \frac{\alpha_{\rm em} y_N^4}{64\pi^2 m_N^2} \left(\frac{7}{2} - \frac{\pi^2}{3} \right), \tag{II.19}$$

with the mass ratio $\mu_N = 1$. This cross section is constrained by the current gamma-ray experiments such as Fermi-LAT [6] and H.E.S.S. [62], and we take the bound which has been obtained in Refs. [55, 63]. The target energy range is 40 GeV to 300 GeV for Fermi-

In this case, further strong gamma-ray emission is expected due to stronger d-wave suppression for 2-body annihilation cross section.

LAT and 500 GeV to 25 TeV for H.E.S.S.. The bound has been obtained by performing a binned profile likelihood analysis and assuming the Einasto profile with the local DM density $\rho_\odot = 0.4$ GeV/cm^3. The data of the gamma-ray flux have been taken from search region 3, Pass7 SOURCE sample for Fermi-LAT as described in Ref. [64], and from CGH region for H.E.S.S. [62] with the expected energy resolution of Fermi-LAT and H.E.S.S. respectively. As mentioned in Ref. [55], the 43 months Fermi-LAT data and the 112h H.E.S.S. data have been analyzed in order to get the bound. Although a similar sharp spectrum of e^+e^- is induced and the model may be constrained by the e^+e^- measurement of AMS-02 [65], this is much weaker than the gamma-ray constraint and does not give a substantial bound.

Here we notice that deviation from $\mu_N = 1$ may weaken the constraint of the gamma-ray in the central region in Fig. 1 because the energy spectrum of gamma-ray coming from internal bremsstrahlung becomes broad. Simultaneously the strong gamma-ray signature of nonthermal DM may not be visible. However another constraint from the LHC arises through the $S^\pm$ production as follows. A pair of the charged scalar $S^\pm$ is produced at the LHC and they decay into $S^\pm \to e^\pm N$ via the Yukawa coupling y_N. This decay width becomes large enough to decay inside the detector if the mass splitting between $S^\pm$ and the DM particle N given by the parameter μ_N deviates from $\mu_N = 1$. As a result, a nontrivial constraint would be obtained, but the situation is beyond our scope. The lower bound for the DM mass obtained from the LHC can be roughly estimated as $m_N \gtrsim 300$ GeV from analogy with the analysis for slepton search in supersymmetric models at the LHC [66].

The white region in Fig. 1 is allowed by all the current experimental and theoretical constraints. From the figure, one can see the allowed region of the X decay width inducing a large Yukawa coupling y_N for the sharp gamma-ray of internal bremsstrahlung is roughly estimated as

$$10^{-22}\ \text{GeV} \lesssim \Gamma_X \lesssim 10^{-16}\ \text{GeV} \quad \text{for} \quad m_X = 1\ \text{TeV}, \tag{II.20}$$

$$10^{-21}\ \text{GeV} \lesssim \Gamma_X \lesssim 10^{-15}\ \text{GeV} \quad \text{for} \quad m_X = 10\ \text{TeV}. \tag{II.21}$$

Thus one can read off the promising parameter region of $\epsilon_1 \equiv \lambda_3 v'/\Lambda$ using Eq. (II.5) as

$$2.2 \times 10^{-12} \lesssim \epsilon_1 \lesssim 2.2 \times 10^{-9} \quad \text{for} \quad m_X = 1, 10\ \text{TeV}. \tag{II.22}$$

	L_L	e_R	X	N	H	η	S^+	S^0
$(SU(2)_L, U(1)_Y)$	$(\mathbf{2}, -1/2)$	$(\mathbf{1}, -1)$	$(\mathbf{1}, 0)$	$(\mathbf{1}, 0)$	$(\mathbf{2}, 1/2)$	$(\mathbf{2}, 1/2)$	$(\mathbf{1}, 1)$	$(\mathbf{1}, 0)$
$(\mathbb{Z}_8,\ \mathbb{Z}_2)$	$(1,\ +)$	$(1,\ +)$	$(1,\ -)$	$(3,\ -)$	$(0,\ +)$	$(0,\ -)$	$(4,\ -)$	$(2,\ +)$
Spin	1/2	1/2	1/2	1/2	0	0	0	0

TABLE II: Particle contents of Model II and their charge assignments under $SU(2)_L \times U(1)_Y \times \mathbb{Z}_8 \times \mathbb{Z}_2$.

III. MODEL II

A. Model setup

Next we discuss Model II, in which the new particle contents and their charge assignments are shown in Table II. In addition to the particle contents of Model I which have been discussed in the previous section, we further add one $SU(2)_L$ doublet inert boson η, and the $\mathbb{Z}_8$ symmetry is imposed instead of the $\mathbb{Z}_4$ symmetry in Model I. This $\mathbb{Z}_8$ symmetry is spontaneously broken by the VEV of S^0, but $\mathbb{Z}_2$ symmetry is the exact symmetry even after the electroweak symmetry breaking. Hence the $\mathbb{Z}_2$ symmetry assures the stability of DM like Model I. We assume that only the SM Higgs denoted as H and the scalar S^0 have VEVs symbolized by $\langle H \rangle = v/\sqrt{2}$, $\langle S^0 \rangle = v'/\sqrt{2}$ respectively.

The relevant Lagrangian up to dimension 5 operators under the above charge assignment is given by

$$\begin{aligned}\mathcal{L} \supset\ & -\frac{y_X}{2} S^{0\dagger} \overline{X^c} X - \frac{y_S}{2} S^0 \overline{N^c} N - y_N S^+ \overline{N^c} e_R - y_\ell H \overline{L_L} e_R - y_\eta \eta^\dagger \overline{L_L} X \\ & - \frac{\lambda_{H\eta}}{2} (H^\dagger \eta)^2 - \frac{1}{2\Lambda} \left(\xi_S S^{0\,2} + \xi'_S S^{0\dagger 2} \right) \overline{N^c} X - \frac{1}{2\Lambda} \left(\kappa_S S^{0\,2} + \kappa'_S S^{0\dagger 2} \right) (\eta H) S^- + \text{H.c.}.\end{aligned} \tag{III.1}$$

The VEV of S^0 gives the masses of the Majorana fermions X and N which are symbolized by $m_N \equiv y_S v'/\sqrt{2}$ and $m_X \equiv y_\chi v'/\sqrt{2}$. The same as Model I, we assume that the Yukawa couplings y_N and y_η only couple with electron for simplicity, and we can naturally expect that the Majorana fermions X and N are almost mass eigenstates since the mixing is generated by the small dimension 5 operators of the ξ_S and ξ'_S terms.

Higgs sector:

Although the CP even neutral scalars with nonzero VEVs (H, S^0) mix with each other the same as Model I, the mixing is not relevant with the following analysis. The charged scalars (η^+, S^+) also mix with each other through the dimension 5 operators including κ_S, κ'_S, and this mixing plays an important role in nonthermal DM production since this mixing leads the decay of X into DM N. The charged scalars η^+ and S^+ are rewritten in terms of the mass eigenstates H_1^+ and H_2^+ as

$$\begin{aligned} \eta^+ &= H_1^+ \cos\theta - H_2^+ \sin\theta, \\ S^+ &= H_1^+ \sin\theta + H_2^+ \cos\theta, \end{aligned} \tag{III.2}$$

where the mixing angle θ is given by

$$\sin 2\theta = \frac{2\epsilon_2 v v'}{m_{H_1}^2 - m_{H_2}^2}, \quad \text{with} \quad \epsilon_2 \equiv \frac{(\kappa_S + \kappa'_S)\, v'}{4\sqrt{2}\Lambda}. \tag{III.3}$$

Lepton sector:

The Weinberg operator $HH\overline{L_L^c}L_L/\Lambda$ is forbidden by the $\mathbb{Z}_8$ symmetry in this model. However, the neutrino masses can be derived at the one-loop level like the Ma model [67]. The neutrino mass formula is given by

$$(m_\nu)_{\alpha\beta} = \sum_i \frac{(y_\eta)_{\alpha i}(y_\eta)_{\beta i} m_{X_i}}{2(4\pi)^2} \left[\frac{m_R^2}{m_R^2 - m_{X_i}^2} \ln\left(\frac{m_R^2}{m_{X_i}^2}\right) - \frac{m_I^2}{m_I^2 - m_{X_i}^2} \ln\left(\frac{m_I^2}{m_{X_i}^2}\right) \right], \tag{III.4}$$

where each of m_R and m_I is the mass eigenvalue of the inert neutral component of the doublet scalar η; η_R and η_I, which is defined in Ref. [67]. The mass difference between η_R and η_I is given by $m_R^2 - m_I^2 = \lambda_{H\eta} v^2$, which is essential to generate nonzero neutrino masses as one can see from the above mass formula. Note that if one requires to reproduce the neutrino oscillation data correctly, at least two kinds of the Majorana fermions X_i are needed as denoted by i in Eq. (III.4). In addition, the constraints from lepton flavor violating processes such as $\mu \to e\gamma$ and $\mu \to e\bar{e}e$ should be taken into account.

B. Dark matter

1. *Relic density*

We assume that the Majorana fermion X is heavier than N the same as Model I. The X decay process $X \to Ne\bar{e}$ is caused by the mixing between the charged scalars as depicted

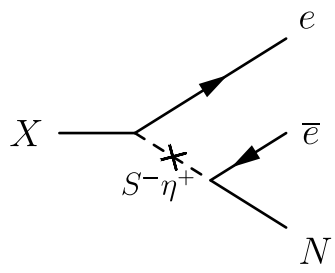

FIG. 2: Decay process of the metastable particle X via the dimension 5 operator.

in Fig. 2. Since the mixing is very small, the fermion X can have a long lifetime like the previous model. However a different point from Model I is that the decaying fermion X is not a FIMP but a normal WIMP which is thermally produced via the renormalizable interaction term y_η. First, the DM particle N is produced by the usual freeze-out scenario, then DM is regenerated by the decay of the metastable fermion X after the freeze-out. Consequently a similar situation with Model I can be realized.

The computation of the DM relic density is discussed below. The coupled Boltzmann equation for X and N is given by [68]

$$\begin{aligned}\frac{dY_X}{dx} &= -\frac{s\langle\sigma_{XX}v_{\rm rel}\rangle}{xH}\left[Y_X^2 - Y_X^{\rm eq2}\left(\frac{m_X}{m_N}x\right)\right] - \frac{\Gamma_X Y_X}{xH},\\ \frac{dY_N}{dx} &= -\frac{s\langle\sigma_{\rm eff}v_{\rm rel}\rangle}{xH}\left(Y_N^2 - Y_N^{\rm eq2}\right) + \frac{\Gamma_X Y_X}{xH},\end{aligned} \tag{III.5}$$

where all the definitions and their values are same with those of the first model. The differential decay width of the decaying particle X for the process $X(p) \to e(k_1)\overline{e}(k_2)N(k_3)$ is calculated as

$$\frac{d\Gamma_X}{dx_E d\Omega}(X \to e\overline{e}N) = m_X \frac{\sqrt{x_E^2 - 4\xi^2}}{(4\pi)^4} \frac{(1 - x_E + \xi^2)\,\overline{|\mathcal{M}|^2}}{\left[2 - x_E + \sqrt{x_E^2 - 4\xi^2}\cos\alpha\right]^2}, \tag{III.6}$$

where the dimensionless parameters ξ and x_E are defined by $\xi = m_N/m_X$, $x_E = 2E_N/m_X$ with the energy of DM E_N and $\cos\alpha$ is the angle between the produced DM and the charged lepton in the final state. The squared amplitude averaged over initial state spin is given by

$$\overline{|\mathcal{M}|^2} = \frac{2\,|y_N y_\eta|^2\,\epsilon_2^2 v^2 v'^2\,(p\cdot k_1)\,(k_2\cdot k_3)}{\left((p-k_1)^2 - m_{H_1}^2\right)^2\left((p-k_1)^2 - m_{H_2}^2\right)^2} + (k_1 \leftrightarrow k_2)\,. \tag{III.7}$$

The total decay width Γ_X can be obtained by integrating Eq. (III.6) in terms of the solid angle Ω and x_E from 2ξ to $1+\xi^2$.

For the annihilation cross sections of X and N, there are various annihilation channels such as $XX, NN \to \ell\bar{\ell}, \nu\bar{\nu}, q\bar{q}, hh, W^+W^-, ZZ$. All the channels except the one into the CP-even Higgs bosons are p-wave dominant which means the cross section is proportional to the relative velocity $v_{\rm rel}^2$. In general, one should include all the channels to compute DM relic density by solving the coupled Boltzmann equation in Eq. (III.5). However in order to find favored parameter space for an interesting gamma-ray signature of nonthermal DM and to simplify our discussion, it is good to assume $y_X, y_S \ll y_N, y_\eta$. In this assumption, the annihilation cross sections for X and N are extremely simplified and become p-wave dominant.[5] The coannihilation processes with the charged scalar $S^\pm$ should also be taken into account since we focus on the degenerate case $m_N \approx m_{S^+}$ for sharp gamma-ray of internal bremsstrahlung. Under the assumption $y_X, y_S \ll y_N, y_\eta$, we can use the same formulas of the (co)annihilation cross sections for DM N with Model I. For the decaying fermion X, the main annihilation process is given by the Yukawa coupling y_η and there are two channels into a pair of the charged leptons and neutrinos since the decaying particle X couples with the left-handed lepton doublet. Thus the cross section $\sigma_{XX} v_{\rm rel}$ is given by

$$\begin{aligned}\sigma_{XX} v_{\rm rel} &= \sigma_{XX} v_{\rm rel}(XX \to e\bar{e}) + \sigma_{XX} v_{\rm rel}(XX \to \nu\nu) \\ &\approx \frac{y_\eta^4}{48\pi m_X^2} \frac{1+\mu_X^2}{(1+\mu_X)^4} v_{\rm rel}^2 + \frac{y_\eta^4}{24\pi m_X^2} \frac{1+\mu_X'^2}{(1+\mu_X')^4} v_{\rm rel}^2, \end{aligned} \tag{III.8}$$

where $\mu_X = m_{\eta^+}^2/m_X^2$ and $\mu_X' = m_{\eta^0}^2/m_X^2$, and the mass difference between η_R and η_I is neglected since it is naturally expected to be small in order to induce the correct neutrino mass scale. The factor 2 difference between the two terms in Eq. (III.8) comes from the Majorana nature of the neutrinos. If we consider the degenerate system such as $\mu_X \approx \mu_X' \approx 1$, the coannihilation processes should be taken into account again. However we do not consider such a case below.

Note that an additional parameter is required for this model compared to Model I as one can see from the Boltzmann equations. In Model I, the DM relic density is determined by the effective cross section $\langle \sigma_{\rm eff} v_{\rm rel} \rangle$ and the decay width Γ_X, while the cross section for the decaying particle $\langle \sigma_{XX} v_{\rm rel} \rangle$ is also needed in Model II. Moreover, one more different point of Model II from Model I is that unlike the FIMP in Model I, the decaying particle X in Model II may be detectable by some experiments through the interaction y_η.

[5] Although more general discussion with $y_X, y_N \sim y_S, y_\eta$ can be done, this is phenomenologically less interesting.

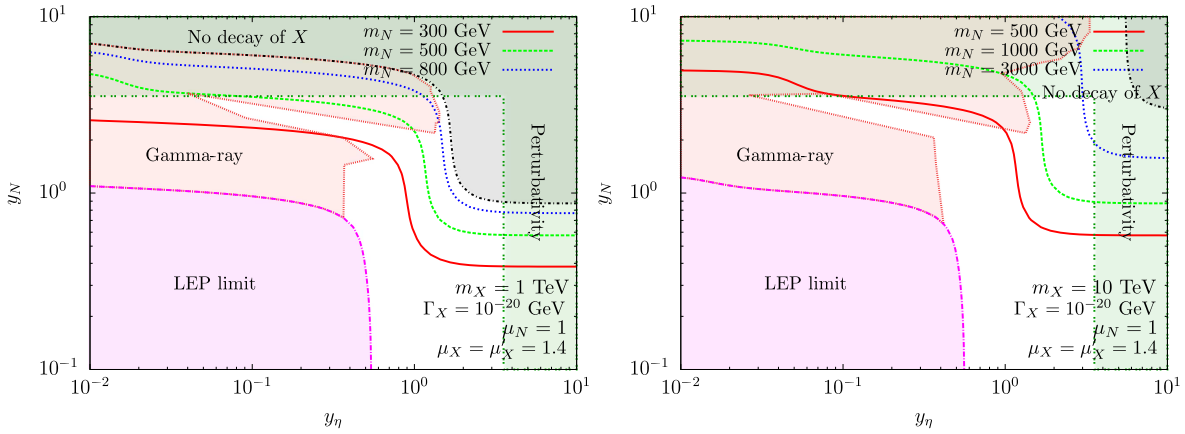

FIG. 3: Allowed parameter space in y_η-y_N plane where the mass of the decaying particle is taken to be m_X =1 TeV in the left panel and m_X = 10 TeV in the right one. The same constraints discussed in Model I such as perturbativity, LEP and gamma-rays are shown together. Only the white region is allowed by all the current experimental and theoretical bounds.

2. *Numerical result*

The Boltzmann equation Eq. (III.5) substituted by Eq (II.18) and (III.8) is numerically solved, and the result is shown in Fig. 3 where the decay width of X is fixed to be $\Gamma_X = 10^{-20}$ GeV, and the mass ratios are fixed to be $\mu_N = 1$ and $\mu_X = \mu'_X = 1.4$ to obtain strong sharp gamma-rays. The X mass is fixed as $m_X = 1$ TeV in the left panel and $m_X = 10$ TeV in the right panel, respectively. The basic setup is the same as that in Model I, and only the white region is allowed by all the current experimental data and theoretical bounds.

From the figure, one can read off the promising parameter range of y_η to see the interesting gamma-ray signal of nonthermal DM which corresponds to $y_N \sim \mathcal{O}(1)$ as

$$0.5 \lesssim y_\eta \lesssim 2.0 \quad \text{for} \quad m_X = 1 \text{ TeV}, \tag{III.9}$$

$$0.5 \lesssim y_\eta \lesssim 3.5 \quad \text{for} \quad m_X = 10 \text{ TeV}, \tag{III.10}$$

for $\Gamma_X = 10^{-20}$ GeV. These ranges are translated to the cross section of the decaying particle X at the freeze-out times as

$$2.9 \times 10^{-11} \lesssim \frac{\langle \sigma_{XX} v_{\rm rel} \rangle}{\text{GeV}^{-2}} \lesssim 7.4 \times 10^{-9} \quad \text{for} \quad m_X = 1 \text{ TeV}, \tag{III.11}$$

$$2.9 \times 10^{-13} \lesssim \frac{\langle \sigma_{XX} v_{\rm rel} \rangle}{\text{GeV}^{-2}} \lesssim 6.9 \times 10^{-10} \quad \text{for} \quad m_X = 10 \text{ TeV}. \tag{III.12}$$

One should note that, for a larger cross section $\sigma_{XX}v_{\rm rel}$, DM is dominated by thermal production and is close to the usual WIMP. In addition, the cross section for the decaying particle X is also bounded from above as $\langle\sigma_{XX}v_{\rm rel}\rangle \lesssim 7.3\times10^{-6}$ GeV^{-2} by the perturbativity limit. Similarly to the case of Model I, deviation from $\mu_N = 1$ emerges the same situation of Model I, but this is beyond our scope.

IV. CONCLUSIONS

From the recent experimental point of view of WIMP searches, the traditional thermally produced WIMP candidate becomes questionable, and a different kind of DM is motivated. We have proposed two kinds of the models, in which DM relic density is generated by nonthermal production mechanisms. The first model includes FIMPs which can decay into DM. Because of the existence of FIMPs, DM is able to be regenerated after the freeze-out and large couplings of DM are allowed compared to usual WIMPs. In the second model, instead of FIMPs, a thermally produced metastable particle is able to decay into DM. Then DM relic density can be mainly produced by the decay of the metastable particle like the first model. In addition, the neutrino masses are generated at the one-loop level.

In these models, we have taken into account some experimental and theoretical constraints such as the DM relic density, the constraints of BBN, collider, gamma-rays and perturbativity of couplings. We have shown the allowed parameter space of the Yukawa coupling which can be translated to the DM annihilation cross section, the decay width of the metastable particle. As a feature of nonthermal DM discussed here, a strong indirect detection signal, especially sharp gamma-rays can be emitted due to internal bremsstrahlung. This would be a promising channel which is testable in future gamma-ray experiments such as CTA, GAMMA-400 and DAMPE.

Acknowledgments

H. O. expresses his sincere gratitude toward all the KIAS members, Korean cordial persons, foods, culture, weather, and all the other things. This work was supported by the Korea Neutrino Research Center which is established by the National Research Foundation of Korea(NRF) grant funded by the Korea government(MSIP) (No. 2009-0083526). T. T.

acknowledges support from P2IO Excellence Laboratory (LABEX).

---

[1] L. Goodenough and D. Hooper, arXiv:0910.2998 [hep-ph].

[2] V. Vitale *et al.* [Fermi-LAT Collaboration], arXiv:0912.3828 [astro-ph.HE].

[3] D. Hooper and T. Linden, Phys. Rev. D **84**, 123005 (2011) [arXiv:1110.0006 [astro-ph.HE]].

[4] K. N. Abazajian, N. Canac, S. Horiuchi and M. Kaplinghat, Phys. Rev. D **90**, no. 2, 023526 (2014) [arXiv:1402.4090 [astro-ph.HE]].

[5] E. Carlson, D. Hooper and T. Linden, Phys. Rev. D **91**, no. 6, 061302 (2015) [arXiv:1409.1572 [astro-ph.HE]].

[6] M. Ackermann *et al.* [Fermi-LAT Collaboration], arXiv:1503.02641 [astro-ph.HE].

[7] D. S. Akerib *et al.* [LUX Collaboration], Phys. Rev. Lett. **112**, 091303 (2014) [arXiv:1310.8214 [astro-ph.CO]].

[8] D. S. Akerib *et al.* [LUX Collaboration], arXiv:1512.03506 [astro-ph.CO].

[9] G. Aad *et al.* [ATLAS Collaboration], Phys. Rev. Lett. **110**, no. 1, 011802 (2013) [arXiv:1209.4625 [hep-ex]].

[10] G. Aad *et al.* [ATLAS Collaboration], JHEP **1304**, 075 (2013) [arXiv:1210.4491 [hep-ex]].

[11] L. Visinelli and P. Gondolo, Phys. Rev. D **80**, 035024 (2009) [arXiv:0903.4377 [astro-ph.CO]].

[12] L. D. Duffy and K. van Bibber, New J. Phys. **11**, 105008 (2009) [arXiv:0904.3346 [hep-ph]].

[13] H. Baer, K. Y. Choi, J. E. Kim and L. Roszkowski, Phys. Rept. **555**, 1 (2014) [arXiv:1407.0017 [hep-ph]].

[14] D. E. Kaplan, M. A. Luty and K. M. Zurek, Phys. Rev. D **79**, 115016 (2009) [arXiv:0901.4117 [hep-ph]].

[15] M. T. Frandsen and S. Sarkar, Phys. Rev. Lett. **105**, 011301 (2010) [arXiv:1003.4505 [hep-ph]].

[16] T. Cohen, D. J. Phalen, A. Pierce and K. M. Zurek, Phys. Rev. D **82**, 056001 (2010) [arXiv:1005.1655 [hep-ph]].

[17] S. Dodelson and L. M. Widrow, Phys. Rev. Lett. **72**, 17 (1994) [hep-ph/9303287].

[18] X. D. Shi and G. M. Fuller, Phys. Rev. Lett. **82**, 2832 (1999) [astro-ph/9810076].

[19] Y. Hochberg, E. Kuflik, T. Volansky and J. G. Wacker, Phys. Rev. Lett. **113**, 171301 (2014) [arXiv:1402.5143 [hep-ph]].

[20] Y. Hochberg, E. Kuflik, H. Murayama, T. Volansky and J. G. Wacker, Phys. Rev. Lett. **115**,

no. 2, 021301 (2015) [arXiv:1411.3727 [hep-ph]].

[21] N. Bernal, C. Garcia-Cely and R. Rosenfeld, JCAP **1504**, no. 04, 012 (2015) [arXiv:1501.01973 [hep-ph]].

[22] S. M. Choi and H. M. Lee, JHEP **1509**, 063 (2015) [arXiv:1505.00960 [hep-ph]].

[23] D. Hooper, F. S. Queiroz and N. Y. Gnedin, Phys. Rev. D **85**, 063513 (2012) [arXiv:1111.6599 [astro-ph.CO]].

[24] Y. Mambrini, K. A. Olive, J. Quevillon and B. Zaldivar, Phys. Rev. Lett. **110**, no. 24, 241306 (2013) [arXiv:1302.4438 [hep-ph]].

[25] T. Moroi, M. Nagai and M. Takimoto, JHEP **1307**, 066 (2013) [arXiv:1303.0948 [hep-ph]].

[26] C. Kelso, S. Profumo and F. S. Queiroz, Phys. Rev. D **88**, no. 2, 023511 (2013) [arXiv:1304.5243 [hep-ph]].

[27] X. Chu, Y. Mambrini, J. Quevillon and B. Zaldivar, JCAP **1401**, 034 (2014) [arXiv:1306.4677 [hep-ph]].

[28] C. Kelso, C. A. de S. Pires, S. Profumo, F. S. Queiroz and P. S. Rodrigues da Silva, Eur. Phys. J. C **74**, no. 3, 2797 (2014) [arXiv:1308.6630 [hep-ph]].

[29] P. S. Bhupal Dev, A. Mazumdar and S. Qutub, Front. Phys. **2**, 26 (2014) [arXiv:1311.5297 [hep-ph]].

[30] G. L. Kane, P. Kumar, B. D. Nelson and B. Zheng, arXiv:1502.05406 [hep-ph].

[31] M. Aoki, T. Toma and A. Vicente, JCAP **1509**, no. 09, 063 (2015) [arXiv:1507.01591 [hep-ph]].

[32] E. Molinaro, C. E. Yaguna and O. Zapata, JCAP **1407**, 015 (2014) [arXiv:1405.1259 [hep-ph]].

[33] M. Blennow, E. Fernandez-Martinez and B. Zaldivar, JCAP **1401**, 003 (2014) [arXiv:1309.7348 [hep-ph]].

[34] P. A. R. Ade *et al.* [Planck Collaboration], Astron. Astrophys. **571**, A16 (2014) [arXiv:1303.5076 [astro-ph.CO]].

[35] L. J. Hall, K. Jedamzik, J. March-Russell and S. M. West, JHEP **1003**, 080 (2010) [arXiv:0911.1120 [hep-ph]].

[36] T. Asaka, K. Ishiwata and T. Moroi, Phys. Rev. D **73**, 051301 (2006) [hep-ph/0512118].

[37] T. Asaka, K. Ishiwata and T. Moroi, Phys. Rev. D **75**, 065001 (2007) [hep-ph/0612211].

[38] M. Berasaluce-Gonzalez, L. E. Ibanez, P. Soler and A. M. Uranga, JHEP **1112**, 113 (2011) [arXiv:1106.4169 [hep-th]].

[39] S. Weinberg, Phys. Rev. D **22**, 1694 (1980).

[40] T. Robens and T. Stefaniak, Eur. Phys. J. C **75**, 104 (2015) [arXiv:1501.02234 [hep-ph]].

[41] F. Elahi, C. Kolda and J. Unwin, JHEP **1503**, 048 (2015) [arXiv:1410.6157 [hep-ph]].

[42] R. Mertig, M. Bohm and A. Denner, Comput. Phys. Commun. **64**, 345 (1991).

[43] A. Pukhov *et al.*, hep-ph/9908288.

[44] A. Pukhov, hep-ph/0412191.

[45] K. Griest and D. Seckel, Phys. Rev. D **43**, 3191 (1991). doi:10.1103/PhysRevD.43.3191

[46] M. Kawasaki, K. Kohri and T. Moroi, Phys. Rev. D **71**, 083502 (2005) [astro-ph/0408426].

[47] K. Jedamzik, Phys. Rev. D **74**, 103509 (2006) [hep-ph/0604251].

[48] LEPSUSYWG, ALEPH, DELPHI, L3 and OPAL experiments, note LEPSUSYWG/04-01.1, (http://lepsusy.web.cern.ch/lepsusy/Welcome.html).

[49] P. J. Fox, R. Harnik, J. Kopp and Y. Tsai, Phys. Rev. D **84**, 014028 (2011) [arXiv:1103.0240 [hep-ph]].

[50] L. Bergstrom, Phys. Lett. B **225**, 372 (1989).

[51] R. Flores, K. A. Olive and S. Rudaz, Phys. Lett. B **232**, 377 (1989).

[52] T. Bringmann, L. Bergstrom and J. Edsjo, JHEP **0801**, 049 (2008) [arXiv:0710.3169 [hep-ph]].

[53] P. Ciafaloni, M. Cirelli, D. Comelli, A. De Simone, A. Riotto and A. Urbano, JCAP **1106**, 018 (2011) [arXiv:1104.2996 [hep-ph]].

[54] V. Barger, W. Y. Keung and D. Marfatia, Phys. Lett. B **707**, 385 (2012) [arXiv:1111.4523 [hep-ph]].

[55] M. Garny, A. Ibarra, M. Pato and S. Vogl, JCAP **1312**, 046 (2013) [arXiv:1306.6342 [hep-ph]].

[56] J. Kopp, L. Michaels and J. Smirnov, JCAP **1404**, 022 (2014) [arXiv:1401.6457 [hep-ph]].

[57] H. Okada and T. Toma, Phys. Lett. B **750**, 266 (2015) [arXiv:1411.4858 [hep-ph]].

[58] T. Toma, Phys. Rev. Lett. **111**, 091301 (2013) [arXiv:1307.6181 [hep-ph]].

[59] F. Giacchino, L. Lopez-Honorez and M. H. G. Tytgat, JCAP **1310**, 025 (2013) [arXiv:1307.6480 [hep-ph]].

[60] A. Ibarra, T. Toma, M. Totzauer and S. Wild, Phys. Rev. D **90**, no. 4, 043526 (2014) [arXiv:1405.6917 [hep-ph]].

[61] F. Giacchino, L. Lopez-Honorez and M. H. G. Tytgat, JCAP **1408**, 046 (2014) [arXiv:1405.6921 [hep-ph]].

[62] A. Abramowski *et al.* [HESS Collaboration], Phys. Rev. Lett. **110**, 041301 (2013) [arXiv:1301.1173 [astro-ph.HE]].

[63] M. Garny, A. Ibarra and S. Vogl, Int. J. Mod. Phys. D **24**, no. 07, 1530019 (2015) [arXiv:1503.01500 [hep-ph]].

[64] C. Weniger, JCAP **1208**, 007 (2012) [arXiv:1204.2797 [hep-ph]].

[65] M. Aguilar *et al.* [AMS Collaboration], Phys. Rev. Lett. **110**, 141102 (2013). doi:10.1103/PhysRevLett.110.141102

[66] The ATLAS collaboration, ATLAS-CONF-2013-049.

[67] E. Ma, Phys. Rev. D **73**, 077301 (2006) [hep-ph/0601225].

[68] M. Fairbairn and J. Zupan, JCAP **0907**, 001 (2009) [arXiv:0810.4147 [hep-ph]].